Local Time Variation in Land/Ocean Lightning Flash Density as Measured by the World Wide Lightning Location Network

Erin H. Lay[(1)], Abram R. Jacobson[(1)], Robert H. Holzworth[(1)], Craig J. Rodger[(2)], Richard L. Dowden[(3)]

(1) Department of Earth and Space Sciences, University of Washington, Seattle, WA, USA
(2) Department of Physics, University of Otago, Dunedin, New Zealand
(3) LF•EM Research Ltd., 161 Pine Hill Road, Dunedin, New Zealand

Abstract. We study local time variation in high peak current lightning over land versus over ocean by using lightning locations from the World Wide Lightning Location Network (WWLLN). Optical lightning data from the photodiode detector on the Fast On-Orbit Recording of Transient Events (FORTE) satellite are used to determine the relative detection efficiency of the WWLLN for lightning events by region, as well as over land versus over ocean. We find that the peak lightning flash density varies for the different continents by up to five hours in local time. Because the WWLLN measures lightning strokes with large peak currents, the variation in local time of WWLLN-detected strokes suggests a similar variation in local time of transient luminous events (e.g., elves) and their effects on the lower ionosphere.

1. Introduction

Over the past few decades, rocket flights in the ionosphere [*Kelley et al.*, 1985; *Li et al*., 1991] have detected electric field transients due to lightning strokes at altitudes of 70-400 km, providing the first direct evidence that lightning energy could penetrate the ionosphere. Also, it has been shown that lightning generates whistler wave radiation that can propagate into the outer magnetosphere [*Holzworth et al.*, 1999]. Lightning-generated whistler waves can also interact with electrons in the radiation belts, causing lightning-induced electron precipitation [*Goldberg et al.*, 1986]. Extremely high energy gamma-ray bursts coming from the Earth's atmosphere, now termed terrestrial gamma-ray flashes (TGFs), were first unexpectedly observed by the BATSE instrument on the Compton Gamma Ray Observatory spacecraft [*Fishman et al.*, 1994]. These TGFs are another indication of energetic coupling of lightning with the magnetosphere. Since 2002, the RHESSI spacecraft has detected hundreds of TGFs, which have been used to link lightning strokes and TGFs [*Smith et al.*, 2005]. All these findings show that lightning has the ability to input energy into the ionosphere and magnetosphere globally and motivate the need for a reliable global lightning detection system.

Transient luminous events (TLEs), such as sprites and elves, are evidence of lightning energy coupling with the lower ionosphere via quasi-electrostatic as well as electromagnetic fields, and can cause ionization, heating and optical emissions in the lower ionosphere [*Inan et al.*, 1991; *Tarenenko et al.*, 1992; *Fukunishi et al.*, 1996]. Various models predict the heating and ionization occurring in the lower ionosphere as a result of the interaction between single lightning strokes and the lower ionosphere and are consistent with optical observations of TLEs [*Taranenko et al.*, 1993, *Fernsler and*

Rowland, 1996; *Pasko et al.*, 1997; *Cho and Rycroft*, 1998]. These models indicate that lightning can affect local conductivity and electron density variations due to electron heating and ionization of the lower ionosphere. It has also been proposed that in severe thunderstorms with high flash rates of strong lightning strokes, the time between flashes could be smaller than the decay time of 10-100 seconds for ionization changes in the lower ionosphere, allowing ionization increases to accumulate in the lower ionosphere locally [*Barrington-Leigh and Inan*, 1999]. *Rodger et al*. [2001] modeled the accumulated increase in electron density as up to a ten-fold increase in the nighttime lower ionosphere.

To better study these energetic effects due to lightning on a global scale, global lightning detection is needed. During the past decade, satellite optical lightning imagers, the Optical Transient Detector (OTD) [*Boccippio et al.*, 2000a] and the Lightning Imaging Sensor (LIS) on the Tropical Rainfall Measuring Mission (TRMM) satellite [*Christian et al.*, 1999] have provided a meaningful global map of average lightning occurrence. Several years of observations have allowed lightning seasonal and local-time variations to be statistically separated, resulting in a comprehensive lightning distribution versus local time, season, and geographic position [*Christian et al.*, 2003; *Boccippio et al*., 2000b; *Petersen and Rutledge* 2001]. *Nesbitt and Zipser* [2003] have used data from the TRMM satellite to study the diurnal cycle of precipitation features over land and ocean. However, the infrequency of satellite observations over a given point, and the precession of the satellite's orbit, together, cause years of cumulative data to be required to separate local-time variability from other changes, such as seasonal and geographic effects. In the interest of studying variabilities on a daily basis and in connection to

certain storms, real-time detection is also important. Ground-based regional detection systems, such as the National Lightning Detection Network (NLDN) in the U.S. [*Cummins et al.*, 1998], provide detailed information about lightning strokes in real-time, but only for limited areas on Earth.

Low-frequency (LF; 30-300 kHz) electromagnetic lightning-detection systems, such as NLDN, tend to be run in a mode that intentionally selects against ionospheric-reflected signals, so that such systems tend not to accept maritime lightning more than several hundred kilometers away from land. Satellite-based very-high-frequency (VHF; 30-300 MHz) lightning detection has been implemented on two small research satellites [*Holden et al.*, 1995; *Massey et al.*, 1998; *Jacobson et al.*, 1999] which cannot by themselves provide accurate lightning location. It is possible that the developmental VHF lightning-detection capability on the GPS constellation [*Suszcynsky et al.*, 2000a] will provide unbiased, global, real-time lightning-incidence maps in the near future, but such capability is not yet available.

Recent developments in very-low-frequency (VLF; 3-30 kHz) electromagnetic lightning detection now allow this technology to detect both continental and oceanic lightning with comparable efficiency. In particular, the World Wide Lightning Location Network (WWLLN) monitors global lightning in real-time [*Dowden et al.*, 2002; *Lay et al.*, 2004; *Rodger et al.*, 2004, 2005]. VLF lightning monitoring with WWLLN is intrinsically long range, because it takes advantage of, rather than rejects, long-range propagation paths in the Earth-ionosphere waveguide. The waveguide propagation paths available in VLF allow useful detection over 10^4 km.

The WWLLN can be used to enhance the understanding of effects of strong lightning strokes on a real-time, global basis. The WWLLN could allow models of the global circuit return current [*Hays and Roble*, 1979] to more accurately predict global circuit behavior in conjunction with real-time measurements of the fair-weather return current [*Holzworth et al*., 2005]. WWLLN global coverage could also be used to study strong lightning activity in conjunction with detected elves, sprites, and TGFs on a global scale.

Before we can begin to apply WWLLN data to these problems, the WWLLN data must be validated in a global manner. In this report we describe a systematic check of the long-range VLF relative detection efficiency over land and over ocean, and over diverse geographical regions, using the FORTE satellite photodiode detector (PDD) optical measurements of lightning as a reference. Although comparisons of the WWLLN to ground-based networks have determined its detection efficiency over small geographic regions, the detection efficiency of WWLLN has not yet been determined on a global scale. Given that the WWLLN VLF receiver stations are not spread exactly uniformly around the world, and that topographical features vary over the earth, the detection efficiency regionally could vary as well. We also study the relative detection efficiency over land and over ocean for the VLF World Wide Lightning Location Network. One might expect a difference in detection efficiency given that lightning-generated VLF radio waves propagate with less attenuation over sea water than over land [*Wait*, 1962]. Since the WWLLN requires that the signal from a lightning sferic be detected by five or more WWLLN VLF stations, a larger attenuation over land could mean that a lightning stroke over land may be less likely to trigger the required five stations.

After presenting the findings of the relative detection efficiency of the WWLLN globally, we then use WWLLN lightning data to examine local time differences in lightning count rate globally and discuss their implications for variations in electron density and conductivity in the lower ionosphere.

2. Data sets

2.1. FORTE photodiode detector

We use optical lightning data from the photodiode detector (PDD) on the Fast On-Orbit Recording of Transient Events (FORTE) satellite [*Suszcynsky et al.*, 2000b, 2001; *Kirkland et al.*, 2001]. The PDD is a non-imaging silicon photodiode collecting light from within a circular field of view of diameter 1200 km at ground level. Because the PDD is non-imaging, any event it detects can be located only to within this 1200-km footprint. The PDD is triggered by a rising optical signal intensity. Once that level exceeds the threshold level and a trigger occurs, a 128-sample register is stored in memory, including 32 samples preceding and 96 samples following the trigger. The sample step is 15 μs, so the record duration is about 1.9 ms. The FORTE satellite is in a 70-degree-inclined, circular orbit at 800 km altitude. Thus the PDD "spotlight" sweeps out the entire region where lightning is found on Earth.

Because the PDD instrument is satellite-based, it observes lightning from above, meaning that it can only detect light that manages to escape from the cloud tops. Previous studies have shown that the majority of PDD-detected events are in-cloud (IC) lightning [*Susczynsky et al*., 1999], although the PDD is also able to detect scattered light from the in-cloud portion of a cloud-to-ground (CG) lightning stroke [*Susczynsky et al*., 2000b].

It has been shown that PDD has a detection efficiency lower than, but constant relative to, LIS detection efficiency over all areas of the world [*Light et al*., 2003]. Thus, we are confident that PDD data serve as an adequate proxy for LIS or OTD data, with the proviso that the PDD locates lightning only to within the 1200-km-diameter field of view, as opposed to within an individualized pixel of an imager. An advantage of PDD for this study is that we can examine optical waveforms relative to the VLF lightning trigger. For this study we assume equal PDD detection efficiencies for land and ocean.

2.2. The World Wide Lightning Location Network

The WWLLN provides real-time lightning locations globally by detecting, from 28 stations world wide, the VLF radiation emanating from lightning discharges. For a lightning stroke to be accurately detected with error analysis, the VLF radiation from the stroke is required to be detected at a minimum of 5 of these 28 receivers. Each receiver locally processes a stroke's waveform and sends the time of group arrival to the central processing station for location [*Dowden et al*., 2002]. In this manner, the WWLLN provides continuous lightning detection coverage of the entire globe.

The location accuracy and efficiency of the WWLLN have been estimated for certain regions by comparison to regional, ground-based lightning detection systems [*Lay et al.*, 2004; *Rodger et al.*, 2005; *Jacobson et al*., 2006; *Rodger et al*., 2006]. *Rodger et al.* [2005] completed a comparison of WWLLN data in Australia to the local Australian lightning location network, Kattron, and found a detection efficiency of ~26% of CG strokes in Australia and ~10% of IC strokes, with a location error of 4.2 ± 2.7 km. By comparison to the Los Alamos Sferic Array (LASA) in the southeastern U.S., *Jacobson*

et al. [2006] found that WWLLN detects ~4% of all strokes, CG and IC, with peak current greater than ~30 kA, and detects with a spatial accuracy of ~15 km. Of the coincident events between WWLLN and LASA, 26% were IC lightning. *Rodger et al.* [2006] found a similar result by comparison to the New Zealand Lightning Detection Network (NZLDN) of a flat detection efficiency for strokes with peak currents larger than ~40 kA.

These previous comparisons to ground-based networks have provided essential information regarding location and timing accuracy of the WWLLN. However, we cannot study the efficiency of WWLLN on a global scale using ground-based networks as a reference. Thus, the comparison of WWLLN-located lightning strokes to optically-detected waveforms measured by the FORTE-PDD instrument is the first global comparison using the WWLLN data set and is intended to verify the relative detection efficiency of WWLLN, in all regions, and over land versus over ocean. After the verification of the relative detection efficiency, we can expand our analysis to the entire WWLLN data set, as opposed to being limited by WWLLN events coincident with PDD-measured optical events.

3. WWLLN/PDD comparison

3.1. Methodology

In this study we search for coincident lightning events between WWLLN-detected lightning sferics and PDD-detected optical waveforms measured between 1 August 2003 and 31 December 2005. To find coincident events, we first exclude any WWLLN events that occur outside the PDD 1200-km field of view. From this reduced WWLLN data set,

we compare the WWLLN sferic time to the optical trigger time. All PDD events that are within 200 milliseconds of a WWLLN-located sferic are corrected in time for the optical signal delay to the satellite, by assuming the WWLLN sferic location as truth. A histogram of the corrected time differences of WWLLN-measured sferic time minus optical trigger time is shown in Figure 1. Figure 1 peaks at -0.25 ms, indicating that the sferic time usually precedes the optical trigger by about 0.25 ms. From this histogram, we choose a classification for coincident events as pairs having a corrected time difference for sferic-optical trigger time between -0.80 ms to 0.30 ms. We choose these limits so that the number of random coincidences occupying the coincidence region is less than 2% of the total: The random coincidence rate of ~20 counts per bin can be seen on the far edges of Figure 1 (absolute value of time differences > 3 ms). Using the random coincidence rate of 20 counts per bin and the total number of coincidences in the region between -0.80 ms to 0.30 ms, we find the number of random coincidences does not exceed 2% of the total.

3.2. Results

In the time period of the comparison, the PDD instrument on FORTE measured 2,520,211 optical events, while WWLLN located 26,430 lightning strokes within the PDD footprint. Of the total number of WWLLN and PDD events, 11,032 participate in a coincident pair. In comparison to earlier WWLLN coincidence studies, this number of pairs is 55 times larger than the comparison by *Lay et al.* [2004] and about 2 times larger than the analysis by *Rodger et al.* [2006].

To examine regional differences in the WWLLN detection efficiency, we separate these events into the six global regions shown in Figure 2. Table 1 shows the results of this categorization. The data are divided into six columns corresponding to the six global regions of interest. The first and second rows show the number of PDD events and WWLLN events, respectively, in each regional box. The third row shows the number of coincident events in each region. The fourth row shows relative detection efficiencies (the total number of WWLLN events detected divided by the total number of PDD events detected) and the fifth row shows the fraction of WWLLN events in each region that were coincident with a PDD event.

One must note that the values shown in Table 1 do not represent absolute detection efficiencies, since, in general, the PDD instrument detects mainly IC lightning while the WWLLN detects mainly CG lightning. In a comparison of PDD to NLDN, which estimates a detection efficiency of ~90% for high peak current strokes, *Suszcynsky et al.* [1999] found that the PDD only detected 5.5% of NLDN-detected negative CG lightning and 8.3% of positive CG lightning. However, even without an absolute detection efficiency calibration, this analysis can provide an understanding of the relative detection efficiency of the WWLLN on a global scale.

The region with the highest detection efficiency is Australasia (region 6), and the lowest detection efficiency is in Europe (region 2), followed by Africa (region 5). The fraction of WWLLN strokes that are coincident with PDD events (row 5 in Table 1) does not correspond directly to the detection efficiency. The lowest fraction is once again in region 2 (Europe), but the highest fraction is now in region 5 (Africa). This difference may mean that the strokes that are detected by PDD in Africa are more likely to be the

type of stroke that also is detected by the WWLLN (high-peak current CG strokes). Since the original submission of this paper, the year 2006 has ended, so we have been able to analyze data from 2006 for these 6 regions. In 2006, WWLLN stations were added in Honolulu, Hawaii; Rothera, Antarctica; Kingston, Australia; Cordoba, Argentina; Ascension Island; and Lanzhou, China. These additions have increased the detection efficiency, as compared to PDD, by 20% overall, and regionally by ~100% in Region 1, ~50% in Region 4, and ~10% in Region 5.

To examine land/ocean differences in the WWLLN detection efficiency, we separate these events into land and ocean subsets in two ways. In the absence of a coincident WWLLN-located lightning stroke, PDD events can be located only to within the 1200-km-diameter PDD footprint, meaning that an optical event detected with the subsatellite point located within 600 km of the coastline could have occurred over either the land or ocean. Therefore, the first classification (shown in Table 2) labels events as "over land" (1st column, Table 2) only if either the WWLLN location, or the FORTE subsatellite point, is over land *and* more than 600 km from the coastline, and labels events as "over ocean" (2nd column, Table 2) only if either the WWLLN location, or the FORTE subsatellite point, are over ocean *and* more than 600 km from the coastline. The lightning "within 600 km of coast" (3rd column, Table 2) is all the remainder and corresponds to lightning that occurred over any surface within 600 km of coast. Most of the lightning-prone areas of Australasia and central America are swept into the coastal category in Table 2. This classification scheme provides us a basis to compare land/ocean differences for all PDD and WWLLN events, as opposed to only coincident events.

In addition to showing lightning counts in the three categories described above, Table 2 also includes a "total" column to provide a quick reference to the total number of PDD and WWLLN events that were detected within the PDD "spotlight" during the time period of the study. We find the ratio of total number of WWLLN events to total number of PDD events over land and ocean in the last row of Table 2. WWLLN detects 0.7% of the number of events PDD detects over land and 0.8% over ocean, indicating a difference of less than 13% in WWLLN detection efficiency over land and over ocean. The ratio of total coastal WWLLN to total coastal PDD events is slightly higher, at 1.2%. We believe this increased ratio can be explained thus: the number of events within 600 km of the coastline is dominated by lightning in Australasia, as most of the land in that region is not more than 600 km from a coastline, and Australasia is the region of highest WWLLN detection efficiency as seen in Table 1.

Next, we focus on coincident events measured by PDD and WWLLN. For this second grouping of data, we take advantage of the more accurate WWLLN location in analyzing events by first assigning each PDD event coincident with a WWLLN event with the location of that WWLLN event. Because WWLLN-measured strokes have a location accuracy of 15-20 km, we next sort coincident events into land and ocean subsets with only a ~50-km-semi-width "coastal" region. The land/ocean/coastal separation map was created using high-resolution continental borders, including major islands, on a 1440×900 pixel grid, covering –70 to 70 degrees latitude. The pixels covering land areas were given a value of 1 and those covering ocean were given a value of 0. A smoothing procedure over 4 pixels gives any land or ocean within 2 pixels of the coastline a value in between 0 and 1, and it is these pixels that are classified as coastal. At

the equator, this gives a coastal area of ~55 km from the coast. Therefore, islands smaller than ~110 km will not be included in the 'land' category. The continental border thickness in Figure 2 indicates the width of the coastal region in this study. WWLLN events located in the coastal region are not used in the land/ocean local time study (section 4), but are included in Table 3 as coastal events. The 50-km-semi-width swath of rejected data additionally allows us to reduce the occurrence of erroneously classifying an oceanic lightning event as over land (or vice versa) due to the 15-20 km location accuracy of WWLLN [*Lay et al*., 2004; *Rodger et al*., 2004; *Jacobson et al*., 2006].

Table 3 shows the results of this stratification. The 1st row shows the number of coincident events, separated into "over land", "over ocean", and "coastal" events by using the criteria described in the previous paragraph. In the second row of Table 3, all WWLLN data are also separated into the three categories using the 50-km-semi-width "coastal" region. The bottom row shows the total number of coincident events divided by the total number of WWLLN events. These results show that 38.9% of WWLLN events over land participate in a coincidence with a PDD event, while 44.4% of oceanic WWLLN events participate in a coincidence. The small percentage difference in land/ocean coincidence detection efficiency indicates that it is unlikely that the WWLLN will completely miss a storm with lightning of similar magnitude over ocean relative to over land. With these statistics, we can begin to use the WWLLN to study relative differences in the effects of strong lightning over land versus over ocean.

A superposed-epoch accumulation of the optical waveform and the sferic stroke time has been performed to further validate the comparison. Figure 3 shows the median, 75th percentile, and 25th percentile amplitudes of all PDD waveforms which participated

in a coincidence with WWLLN. The amplitudes are considered separately in each time bin. The waveforms are shifted in time to position the WWLLN-calculated sferic time at 0.00 seconds. The 0.3- to 0.4-ms delay in the optical peak is slightly longer than found by *Susczynsky et al.* [2000b] in a VHF/optical comparison, in which a 243-μs average delay of the optical peak was attributed to a 105-μs average delay between VHF and optical emission plus an average 138-μs broadening due to scattering delay of light in its travel through the cloud. Figure 3 shows general agreement with the timing data and waveform shapes of previous studies, giving cause to trust the coincidences found by this comparison.

With confidence in the WWLLN/PDD-detected coincidences and in the relative detection efficiency of WWLLN over land and ocean, we can use the entire, not just PDD-coincident, WWLLN data set to look at land/ocean effects in high peak current lightning occurrence. In the remainder of this paper, we will look at local time differences in lightning over land and over ocean and demonstrate the suitability of WWLLN as a tool to study these variations on shorter time scales than can be seen from satellite averages.

4. Land/ocean events in local time

Using WWLLN data from 2005, we will show that the WWLLN local time variations of flash density are consistent with previous satellite and regional ground-based studies, and can be used as a tool to further study the land/ocean diurnal cycle of lightning in real-time or over a short time scale. Figure 4 indicates that WWLLN data, taken over one year and the entire globe, shows a peak in lightning over land in the local

afternoon around 1800 local time, and shows that the diurnal cycle of oceanic lightning, while having a much smaller amplitude than that of land lightning, peaks in the morning around 0800 local time. Local time for each stroke is defined as local solar time at the location of the lightning stroke. This global study shows that the annually averaged WWLLN diurnal variation is consistent with previous studies using satellite optical detectors: *Williams et al.* [2000] show lightning counts over land peak around 1600 local time while lightning counts over ocean remain relatively constant throughout a local day. *Nesbitt and Zipser* [2003] find precipitation features indicating high levels of convection and possibly lightning peak in number around 1500 local time over land, while these precipitation features over ocean have a smaller amplitude in their diurnal cycle and peak in the local morning, around 0500-0700 local time.

In addition, WWLLN's real-time global coverage can separate the effects on the diurnal variation of separate continental bodies, seasonal effects, and individual storms. The capabilities of this continuous global lightning data will be useful in conjunction with recent and future data recorded by satellites viewing TLEs and TGFs. Lightning detection satellites view small regions on Earth at any given time, so it is unlikely that they will be viewing the same region at the same time as the TLE and TGF-detecting satellites.

To demonstrate the capability of the WWLLN to study diurnal lightning variation of geographic regions, in Figure 5 we separate the data from Figure 4 into the same six regions as used in Figure 2. Figure 5 shows the contribution each region makes to the position of the local time peak in lightning flash density. The flash density in each region varies based on the strength of the region in producing lightning as well as the WWLLN

detection efficiency in that region. For example, the WWLLN has the highest detection efficiency in Australasia (region 6), so the lightning flash density is high for that region. Detection efficiency is lower in Africa (region 5), but Africa has the highest flash density of all the regions [*Christian et al.*, 2003], so the WWLLN flash density is also high in that region. The local afternoon peak in land lightning flash density is evident in all regions, but shifted slightly based on region. To better represent the relative positions of the peak, Figure 6 shows land lightning data for all six regions on the same plot, normalized to the same peak amplitude. As the peaks are fairly broad, the center of a full-width-half-max (FWHM) estimate is marked at the top of Figure 6, with region number labeling each adjusted peak. Land lightning over Europe (region 2) peaks earliest, around 1500 local time, while land lightning over North America (region 1) peaks latest, around 1900 LT. The time of peak lightning flash density over North America is consistent with findings from 5-year and 10-year averaged NLDN data that indicate that, in areas of the U.S. with significant diurnal variation, peak lightning flash rates occur between 1600 and 2000 LT [*Zajac and Rutledge*, 2000; *Orville and Huffines*, 2001]. Both these studies looked at geographic effects on a much finer scale and determined that orography and local continental weather patterns have a large effect on the time of the peak lightning flash rate. Variations in the local time of peak lightning flash rates for the regions presented in this paper may also be due to differing continental weather patterns. WWLLN data could also be used to study smaller-scale variations in any region of the world, although we leave this study for future work.

Figures 4, 5 and 6 show that the WWLLN is consistent with previous studies over long durations and can provide new information about geographic effects on high peak

current lightning. Moreover, the WWLLN has the advantage of real-time global coverage that satellites cannot achieve, meaning that WWLLN can be used to look for local time variations in the high peak current lightning flash density on shorter time scales. Figure 7 shows that the WWLLN can provide a meaningful picture of local time variation in lightning count rates on a five-day time scale. Global lightning flash density, in 15-minute local time bins and separated into land and ocean events, is plotted for 1-5 January 2005 in Figure 7a and 1-5 July 2005 in Figure 7b. The global five-day interval was chosen to illustrate the capability of the WWLLN in studying small time scale variabilities, but essentially any interval of time in any region could be analyzed.

By plotting WWLLN flash density versus local time, we see regional differences in the location of the peak lightning flash density in local time. Previous studies have shown that WWLLN detects large peak current lightning strokes [*Lay et al*., 2004; *Rodger et al*., 2005; *Jacobson et al*., 2006]. *Barrington-Leigh and Inan* [1999] reported that all CG lightning strokes with peak currents larger than ~50 kA produce doughnut-shaped optical emissions called elves in the lower ionosphere through lightning-generated electromagnetic pulse (EMP). Thus, this local time study of WWLLN strokes over land and ocean effectively shows the regional local time variation of large lightning strokes and therefore elves. The late temporal peak of lightning over land in North America indicates that many large peak current strokes occur under the nighttime ionosphere, where the lightning EMP has a long-lasting effect in the D-layer ionization [*Rodger et al*., 2001]. We can use lightning count rates in local time to estimate the fraction of elves-producing lightning that occurs under the nighttime ionosphere in each region. We will define the time of the nighttime ionosphere from 1800-0600 LT. Figure 8 shows this

fraction in each region. More than 60% of lightning in regions 1 and 4 (North and South America) occurs under the nighttime ionosphere, where high peak current lightning strokes can have a long-lasting effect in the D-layer ionization. In contrast, only ~43-44% of lightning in regions 1 and 3 (Asia and Australasia) occurs under the nighttime ionosphere. This ~20% difference suggests high peak current lightning in the Americas may input a more significant amount of energy into the nighttime ionospheric D-region than would Asia and Australia.

5. Conclusion

Local time studies of WWLLN lightning data show that peak flash density of strong lightning varies for the different continents by up to five hours in local time. We have suggested that WWLLN data can give an indication of the local time distributions of effects from strong lightning strokes, such as elves, sprites, and electron density and conductivity variability in the lower ionosphere. These variations can be monitored in real-time and could be important to include in models of the global electric circuit.

The presented comparison of the World Wide Lightning Location Network with satellite optical data has provided global verification of the capabilities of the WWLLN in detecting lightning globally and over land versus ocean with a similar relative detection efficiency. The WWLLN is shown to have the ability to address questions regarding land/ocean lightning differences in local time on any time scale in any location on Earth. WWLLN data could be useful for researchers trying to verify lightning count rates during short campaigns, or, as is commonly the case, during a time when low-Earth orbiting optical lightning satellites are not viewing the regional area of interest.

Acknowledgements

The University of Washington would like to acknowledge NSF grant ATM-0355190 and the Mindlin Foundation for supporting this research.

References

Barrington-Leigh, C.P. and U.S. Inan. (1999), Elves triggered by positive and negative lightning discharges. *Geophys. Res. Letters, 26*, 6, 683-686.

Boccippio, D. J., W. J. Koshak, H. J. Christian, and S. J. Goodman (1999), Land-ocean differences in LIS and OTD tropical lightning observations. 11th International Conference on Atmospheric Electricity, Global Hydrology and Climate Center, NASA Marshall Space Flight Center, Huntsville, Alabama.

Boccippio, D. J., K. Driscoll, W. Koshak, R. Blakeslee, W. Boeck, D. Buechler, H. Christian, and S. Goodman (2000a), The Optical Transient Detector (OTD): Instrument characteristics and cross-sensor validation. *J. Atmos. Oceanic Tech.*, *17***,** 441-458.

Boccippio, D. J., S. J. Goodman, and S. Heckman (2000b), Regional differences in tropical lightning distributions. *J. Appl. Meteor.*, *39***,** 2231-2248.

Cho, M and M.J. Rycroft (1998), Computer simulation of the electric field structure and optical emission from cloud-top to the ionosphere, J. of Atmos. and Solar-Terr. Phys., 60, 871-888.

Christian, H. J., R. J. Blakeslee, S. J. Goodman, D. A. Mach, M. F. Stewart, D. E. Buechler, W. J. Koshak, J. M. Hall, W. L. Boeck, K. T. Driscoll, and D. J. Boccippio (1999), The Lightning Imaging Sensor. 11th International Conference on Atmospheric Electricity, Global Hydrology and Climate Center, NASA Marshall Space Flight Center, Huntsville, Alabama.

Christian, H. J., R. J. Blakeslee, D. J. Boccippio, W. L. Boeck, D. E. Buechler, K. T. Driscoll, S. J. Goodman, J. M. Hall, W. J. Koshak, D. M. Mach, and M. F. Stewart (2003), Global frequency and distribution of lightning as observed from space by the Optical Transient Detector, *J. Geophys. Res.*, *108*(D1), 10.1029/2002JD002347.

Cummins, K. L., M. J. Murphy, E. A. Bardo, W. L. Hiscox, R. Pyle, and A. E. Pifer (1998), Combined TOA/MDF technology upgrade of U. S. National Lightning Detection Network. *J. Geophys. Res.*, *103***,** 9035-9044.

Dowden, R. L., J. B. Brundell, and C. J. Rodger (2002), VLF lightning location by time of group arrival (TOGA) at multiple sites. *J. Atmos. Solar-Terrest. Phys.*, *64***,** 817-830.

Fernsler, R. F. and H. L. Rowland (1996), Models of lightning-produced sprites and elves, *J. of Geophys. Res.,* 101(D23), 29,653-662.

Fishman, G.J., P.N. Bhat, R. Mallozzi, J.M. Horack, T. Koshut, C. Kouveliotou, G.N. Pendleton, C.A. Meegan, R.B. Wilson, W.S. Paciesas, S.J. Goodman, H.J. Christian (1994), Discovery of intense gamma-ray flashes of atmospheric origin, *Science, 264*, 5163: 1313-1316.

Fukunishi, H., Y. Takahashi, M. Kubota, K. Sakanoi, U.S. Inan, W.A. Lyons (1996), Elves: Lightning-induced transient luminous events in the lower ionosphere, *Geophys. Res. Lett.*, *23*, 16, 2157-2160.

Goldberg, R.A., J.R. Barcus, L. Hale, S.A. Curtis (1986), Direct observation of magnetospheric electron-precipitation stimulated by lightning, *J. of Atmos. And Terr. Phys., 48* (3), 293-299.

Hays, P. B. and R. G. Roble (1979), A Quasi-Static Model of Global Atmospheric Electricity. 1. The Lower Atmosphere. *J. of Geophys. Res*. *84*(A7), 3291-3305.

Holden, D. N., C. P. Munson, and J. C. Devenport (1995), Satellite observations of transionospheric pulse pairs. *Geophys. Res. Lett.*, *22***,** 889-892.

Holzworth R. H, R. M. Winglee, B. H. Barnum, Y. Q. Li, and M. C. Kelley (1999), Lightning whistler waves in the high-latitude magnetosphere, *J. of Geophys. Res., 104*, A8, 17369-17,378.

Holzworth, R. H., E. A. Bering III, M. F. Kokorowski, E. H. Lay, B. Reddell, A. Kadokura, H. Yamagishi, N. Sato, M. Ejiri, H. Hirosawa, T. Yamagami, S.Torii, F. Tohyama, M. Nakagawa, T. Okada, and R. L. Dowden (2005), Balloon observations of temporal variation in the global circuit compared to global lightning activity, *Advances in Space Research, 36,11*, 2223-2228.

Inan, U.S., T.F. Bell, J.V. Rodriguez (1991), Heating and ionization of the lower ionosphere by lightning, *Geophys. Res. Lett., 18,* 705-708.

Jacobson, A. R., S. O. Knox, R. Franz, and D. C. Enemark (1999), FORTE observations of lightning radio-frequency signatures: Capabilities and basic results. *Radio Sci.*, *34***,** 337-354.

Jacobson, A. R., R. Holzworth, J. Harlin, R. Dowden, and E. Lay (2006), Performance Assessment of the World Wide Lightning Location Network (WWLLN), Using the Los Alamos Sferic Array (LASA) as Ground Truth, *J. Atmos. and Oceanic Technology*, *23*, 1082-1092.

Kelley, M.C., C.L. Siefring, R.F. Pfaff, P.M. Kintner, M. Larsen, R. Green, R.H. Holzworth, L.C. Hale, J.D. Mitchell, and D. LeVine (1985), Electrical measurements in the atmosphere and the ionosphere over an active thunderstorm. 1. Campaign overview and initial ionospheric results, *J. of Geophys. Res., 90*, A10, 9815-9823.

Kirkland, M. W., D. M. Suszcynsky, J. L. L. Guillen, and J. L. Green (2001), Optical observations of terrestrial lightning by the FORTE satellite photodiode detector. *J. Geophys. Res.*, *106***,** 33,499-33,509.

Lay, E. H., R. H. Holzworth, C. J. Rodger, J. N. Thomas, O. Pinto, Jr., and R. L. Dowden (2004), WWLL Global Lightning Detection System: Regional Validation Study in Brazil, *Geophys. Res. Lett., 31*, L03102, doi: 10.1029/2003GL018882.

Li, Y.Q., R. H. Holzworth, H. Hu, M. McCarthy, R. D. Massey, P. M. Kintner, J. V. Rodrigues, U. S. Inan, and W. C. Armstrong (1991), Anomalous optical events detected by rocket-borne sensor in the WIPP campaign, *J. of Geophys. Res., 96*, A2 1315-1326.

T. E. Light, S. M. Davis, W. Boeck, A. R. Jacobson (2003), Global nighttime lightning flash rates and characteristics observed with the FORTE satellite, *Los Alamos National Laboratory technical report*, LA-UR 03-5909.

Massey, R. S., D. N. Holden, and X.-M. Shao (1998), Phenomenology of trans-ionospheric pulse pairs: Further observations. *Radio Sci*, *33***,** 1755-1761.

Nesbitt, S.W. and E.J. Zipser (2003), The Diurnal Cycle of Rainfall and Convective Intensity according to Three Years of TRMM Measurements. *J. of Climate*, *16*, 1456-1475.

Orville, R.E. and G. R. Huffines (2001), Cloud-to-Ground Lightning in the United States: NLDN Results in the First Decade, 1989–98. Monthly Weather Rev., *129***,** 1179-1193.

Pasko, V.P, U.S. Inan, T.F. Bell, and Y.N. Tarenenko (1997), Sprites produced by quasi-electrostatic heating and ionization in the lower ionosphere, *J. of Geophys. Res., 102*, A3, 4529-4561.

Petersen, W. A. and S. A. Rutledge (2001), Regional variability in tropical convection: Observations from TRMM. *J. Climate*, *14***,** doi:10.1175/1520-0442.

Rodger, C.J., M. Cho, M.A. Clilverd, and M.J. Rycroft (2001), Lower ionospheric modification by lightning-EMP: Simulation of the night ionosphere over the United States. *Geophys. Res. Lett.*, *28*(2), 199-202.

Rodger, C. J., J. B. Brundell, R. L. Dowden, and N. R. Thomson (2004), Location accuracy of long distance VLF lightning location network. *Ann. Geophys.*, *22***,** 747-758.

Rodger, C. J., J. B. Brundell, and R. L. Dowden (2005), Location accuracy of VLF World Wide Lightning Location (WWLL) network: Post-algorithm upgrade. *Ann. Geophys.*, *23***,** 277-290.

Rodger, C. J., S. W. Werner, J. B. Brundell, N. R. Thomson, E. H. Lay, R. H. Holzworth, and R. L. Dowden (2006), Detection efficiency of the VLF World-Wide Lightning Location Network (WWLLN): Initial case study, *Annales Geophys.*, *24*, 3197-3214.

Smith, D.M., L.I. Lopez, R.P. Lin, C.P. Barrington-Leigh (2005), Terrestrial gamma-ray flashes observed up to 20 MeV, *Science,* 307, 5712, 1085 – 1088, DOI: 10.1126/science.1107466.

Suszcynsky, D. M., M. Kirkland, P. Argo, R. Franz, A. Jacobson, S. Knox, J. Guillen, J. Green, and R. Spalding (1999), Thunderstorm and lightning studies using the FORTE optical lightning system (FORTE/OLS), *Proceedings of the 11th International Conference on Atmospheric Electricity*, edited by H. Christian, *NASA/CP-1999-209261*, 672-675.

Suszcynsky, D., A. Jacobson, J. Fitzgerald, C. Rhodes, E. Tech, and D. Roussel-Dupre (2000a), Satellite-based global lightning and severe storm monitoring using VHF receivers. *EOS, Trans. Am. Geophys. Union*, *81***,** F91.

Suszcynsky, D. M., M. W. Kirkland, A. R. Jacobson, R. C. Franz, S. O. Knox, J. L. L. Guillen, and J. L. Green (2000b), FORTE observations of simultaneous VHF and optical emissions from lightning: Basic Phenomenology. *J. Geophys. Res.*, *105***,** 2191-2201.

Suszcynsky, D. M., T. E. Light, S. Davis, M. W. Kirkland, J. L. Green, and J. Guillen, (2001), Coordinated Observations of Optical Lightning from Space using the FORTE Photodiode Detector and CCD Imager. *J. Geophys. Res.*, *106***,** 17,897-17,906.

Taranenko, Y.N., U.S. Inan, and T.F. Bell (1992), Optical signatures of lightning-induced heating of the D-region, *Geophys. Res. Lett.*, *19 (18)*, 1815-1818.

Tarenenko, Y.N., U.S. Inan, and T.F. Bell (1993), Interaction with the lower ionosphere of electromagnetic pulses from lightning: heating, attachment, and ionization, *Geophys. Res. Lett., 20,* 15, 1539-1542.

Wait, J.R. (1962), *Electromagnetic Waves in Stratified Media*, Pergamon Press Inc., New York.

Williams, E., K. Rothkin, D. Stevenson, and D. Boccippio (2000), Global Lightning Variations Caused by Changes in Thunderstorm Flash Rate and by Changes in the Number of Thunderstorms. *J. of Applied Meterology*, *39*, 2223-2230.

Zajac, B. A. and S. A. Rutledge (2001), Cloud-to-ground lightning activity in the contiguous United States from 1995 to 1999. *Monthly Weather Rev., 129 (5),* 999-1019.

Table 1. Results of WWLLN/PDD regional comparison

Region #	**1**	**2**	**3**	**4**	**5**	**6**
PDD total	232,380	88,474	187,935	480,907	802,771	727,744
wwlln total	2,204	428	1,552	4,198	4,821	13,227
# coincs.	905	161	655	1,692	2,131	5,488
wwlln total / PDD total	0.009	0.005	0.008	0.009	0.006	0.018
# coincs. / wwlln total	0.411	0.376	0.422	0.403	0.442	0.415

Table 2. Results of WWLLN/PDD land/ocean comparison using 600-km coastal areas

	over land & >600km from coast	over ocean & >600km from coast	within 600km of coast	**total**
PDD total	401,902	255,107	1,863,202	**2,520,211**
wwlln total	2,892	2,064	21,474	**26,430**
wwlln/PDD	**0.007**	**0.008**	0.012	**0.010**

Table 3. Results of WWLLN/PDD land/ocean coincidence comparison

	over land	over ocean	coastal	**total**
# coincs.	4,307	4,122	2,603	**11,032**
wwlln total	11,074	9,290	6,066	**26,430**
# coincs. / wwlln total	**0.389**	**0.444**	0.429	**0.417**

Figure Captions

Figure 1. Time-difference histogram of WWLLN-sferic time minus FORTE PDD trigger time, corrected for optical signal delay to satellite. Bin size is 0.0001 second. The peak occurs at ~ -250 μs, indicating that the PDD optical is triggered about 250 μs after WWLLN detects the sferic. The two vertical dashed lines indicate the timing cutoffs for coincident events (-0.80 to 0.30-ms timing difference). 11,032 events fall within the cutoff times.

Figure 2. Diamonds indicate WWLLN station locations in January 2005 while the numbers indicate the six broad regions used in this study. The thickness of the coastlines shows the size of the coastal region used in the land/ocean study.

Figure 3. A superposed epoch of PDD waveforms with WWLLN coincidences. The median (solid line), 75^{th} percentile (dashed-dotted line), and 25^{th} percentile (dotted line) of all PDD waveforms which participated in a 1.1-ms coincidence with WWLLN are separately plotted. These statistics are computed independently for each time bin. The waveforms are individually shifted in time to place the WWLLN-calculated sferic time at 0.00 seconds.

Figure 4. One year (2005) of WWLLN flash density data (in units of 10^{-4} sferics per square kilometer per year), separated into land and ocean events, and plotted versus local time in 15-minute bins. The diurnal amplitude variation of land events is about three times larger than the diurnal amplitude variation in oceanic events. Land events peak in

the local evening, around 1800 LT, while oceanic events peak in the morning, around 0800 LT.

Figure 5. The same year of WWLLN flash density data as shown in Figure 4, now separated into the six broad regions shown in Figure 2. a)-f) show data from regions 1-6, respectively. Similar diurnal patterns are seen in each region. However, the land and ocean peak amplitudes do not occur at the same LT in each region. Poisson statistics define error bars on the order of the width of the line. The largest percentage error occurs in b) where, for example, the error at 14 LT is $\pm$ 0.084 x 10^{-4} sf km^{-2} yr^{-1}.

Figure 6. Land data from the six regions in Figure 5, normalized to unit height and overlaid to observe relative local time positions of the peak amplitude. The center of the FWHM peak for each region is marked at the top of the figure, with region number labeling each adjusted peak. Land flash density in Europe peaks earliest, at 1530 LT, while the land flash density in North America peaks latest, at 1950 LT.

Figure 7. Five days of land/ocean WWLLN flash density data (in units of 10^{-4} sferics per square kilometer per year) from 1-5 January 2005 (a) and 1-5 July 2005 (b). Poisson error bars are on the order of the width of the data line. Using WWLLN, one can study local time variations of lightning during very short time intervals.

Figure 8. Percentage of total lightning in nighttime (1800 – 0600 LT) in each region. More than 60% of lightning in regions 1 and 4 (North and South America) occurs under the nighttime ionosphere, where strong lightning strokes can have a long-lasting effect in the D-layer ionization.

Figure 1.

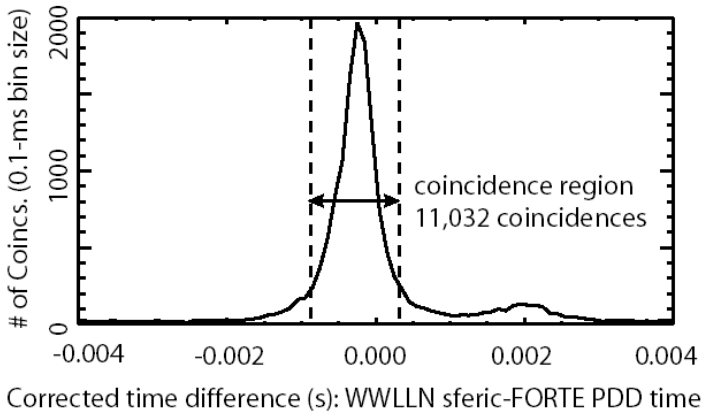

Figure 2.

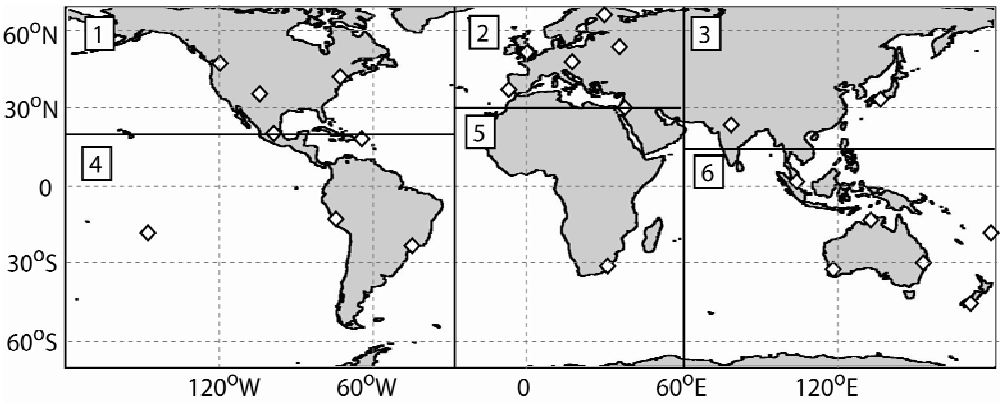

Figure 3.

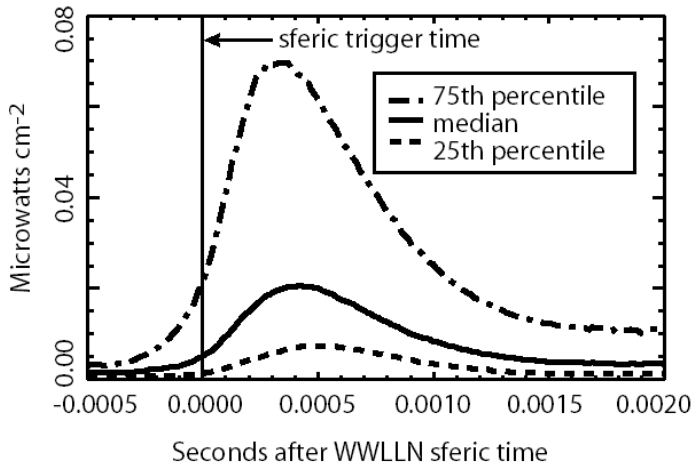

Figure 4.

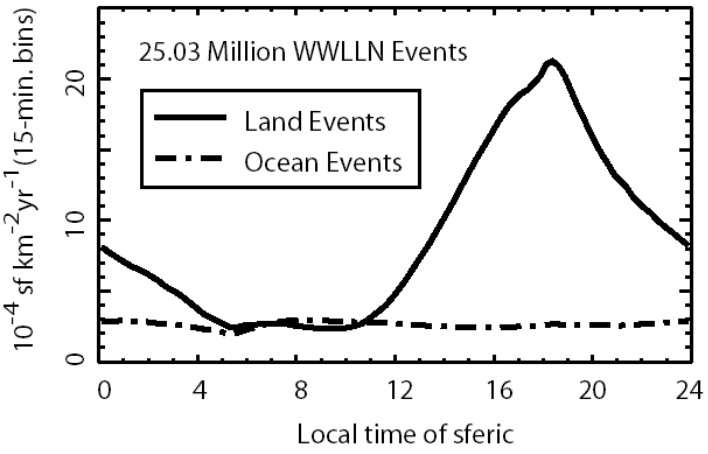

Figure 5.

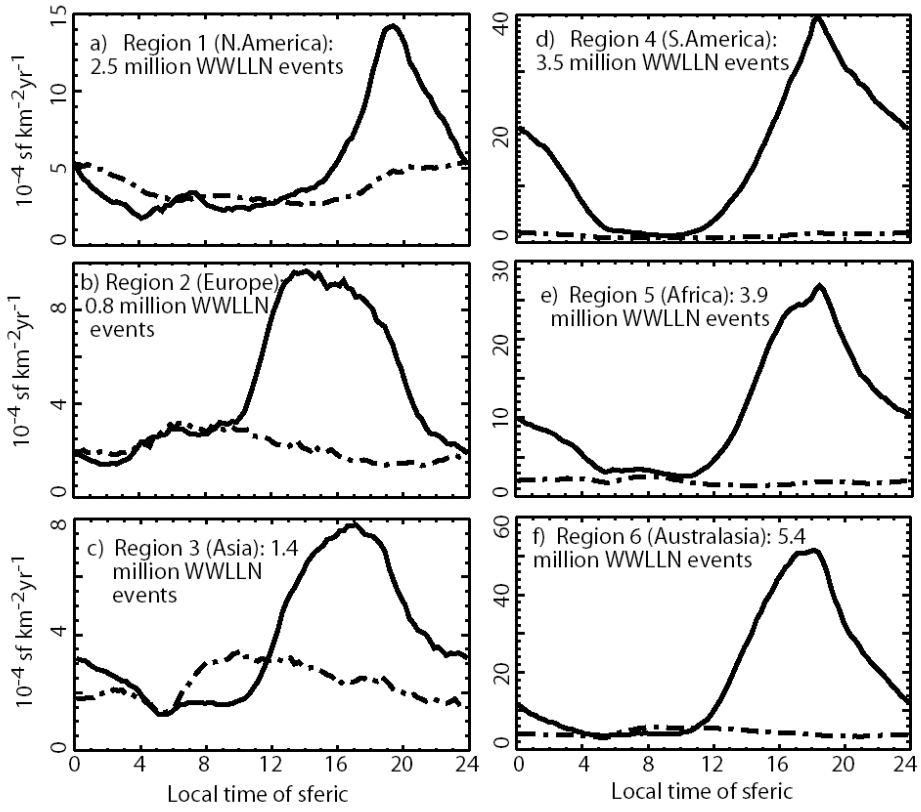
a) Region 1 (N.America): 2.5 million WWLLN events
b) Region 2 (Europe): 0.8 million WWLLN events
c) Region 3 (Asia): 1.4 million WWLLN events
d) Region 4 (S.America): 3.5 million WWLLN events
e) Region 5 (Africa): 3.9 million WWLLN events
f) Region 6 (Australasia): 5.4 million WWLLN events
10^-4 sf km^-2yr^-1
Local time of sferic

Figure 6.

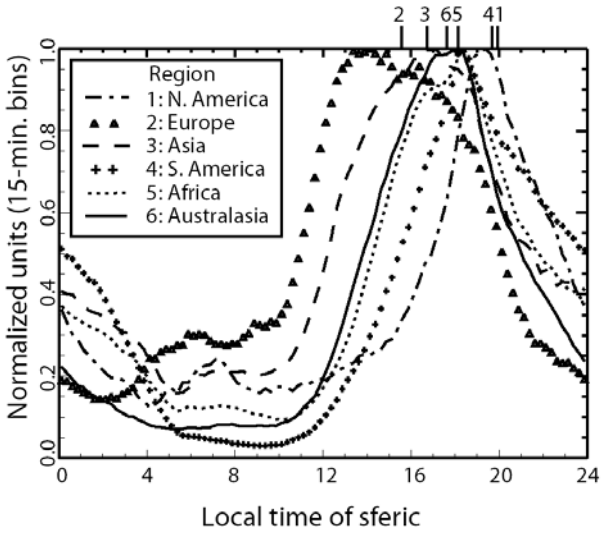

Figure 7.

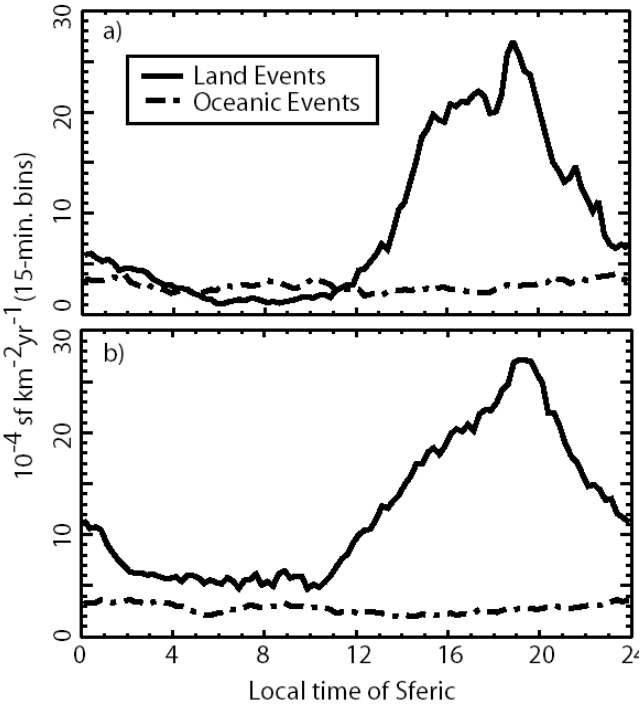

Figure 8.